Table 1. Results of calcite-aragonite experiments: C, calcite; A, aragonite; parentheses denote minor phase. Starting materials: P, precipitated fine calcite and aragonite; M, metamorphic aragonite with minor calcite.

Temp. (°C)	Pressure (kb)	Starting material	Products	Time (days)
109	6.21	P	A	5
120	6.00	P	A+(C)	5
101	5.52	P	A+(C)	5
100	5.18	P	No change	5
110	5.00	P	A+(C)	5
100	4.14	P	C	5
107	4.48	P	A+(C)	14
100	4.83	P	A+(C)	17
115	4.14	P	C+(A)	17
98	4.48	M	A+(C)	20
105	4.14	M	C+(A)	20
105	4.83	M	A	29

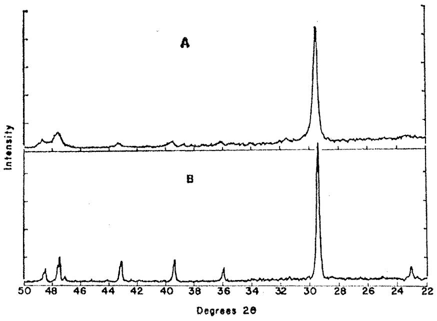

Fig. 1. Comparison of two x-ray diffraction patterns of a fine precipitated calcite. (*A*) After squeezing at 10 kb at room temperature. (*B*) Original material. Note the disappearance and broadening of the lines in *A*.

have repeated these studies in conventional hydrostatic apparatus.

The reaction was studied by placing mixtures of calcite and aragonite in small hot-seal vessels. A small amount of calcium chloride was added to each charge to give an approximately 0.2 molar solution. Calcium chloride greatly accelerates the rate of attainment of equilibrium in this reaction. Charges were brought to temperature dry, and then pumped to the desired pressure. Two starting materials were used and gave identical results. A mixture of fine calcite and aragonite was precipitated at 100°C from potassium carbonate and calcium chloride solutions. The second material was a sample of metamorphic aragonite supplied by R. G. Coleman and described in Coleman and Lee [(*7*), sample 45-CZ-59]. This material contains a small amount of calcite and about 1.11 percent strontium carbonate as the only major impurity. The material was ground to pass a 325-mesh screen. Phases produced and changes in relative quantities were determined by x-ray diffraction and optical observation. The data are given in Table 1. There was no evidence of any contamination of products by calcium chloride solutions nor do mineralogical data of Deer, Howie, and Zussman (*8*) indicate chloride solid solution in these phases.

Inspection of these data indicates a transition pressure between 4.2 and 4.5 kb at 100°C. The results are very close to those of Jamieson, MacDonald, and Clark and indicate that Simmons and Bell's transition pressure is much too high at this temperature.

Some observations on squeezer products are of interest in evaluating the significance of data derived from such apparatus where shearing stresses may be large. In Fig. 1 diffraction patterns are compared for a fine precipitated calcite (*B* in the figure) and the same material after squeezing at 10 kb at room temperature (*A*). The squeezed material shows intense line broadening, a result of some combination of grain size reduction and internal strain, the latter being associated with a large dislocation density. Aragonite squeezed at 10 kb also shows broadening of comparable magnitude. Paterson (*9*) has discussed line broadening in deformed calcite and suggested that the stored strain energy may be of the order of 1000 cal/mole. The broadening in Fig. 1 is far larger than that found by Paterson. The strain energy term may be much larger than the free energy of the calcite-aragonite transition and it may well be necessary to consider exactly what physical state of a system is being studied in shearing apparatus. It certainly does not appear to be that of hydrostatically stressed particles of reasonable grain size.

WILLIAM A. CRAWFORD
WILLIAM S. FYFE
Department of Geology and Geophysics, University of California, Berkeley

References and Notes

1. W. M. Latimer, *Oxidation Potentials* (Prentice Hall, Englewood Cliffs, ed. 2, 1952), p. 320.
2. J. C. Jamieson, *J. Chem. Phys.* **21**, 1385 (1953).
3. G. J. F. MacDonald, *Am. Mineralogist* **41**, 744 (1956).
4. S. P. Clark, Jr., *ibid.* **42**, 564 (1957).
5. F. Dachille and R. Roy, in *Reactivity of Solids*, J. H. De Boer, Ed. (Elsevier, Amsterdam, 1960), p. 502.
6. G. Simmons and P. Bell, *Science* **139**, 1197 (1963).
7. R. G. Coleman and D. E. Lee, *Am. J. Sci.* **260**, 588 (1962).
8. W. A. Deer, R. A. Howie, J. Zussman, *Rock-Forming Minerals* (Wiley, New York, 1963), vol. 5, pp. 232, 397.
9. M. S. Paterson, *Phil. Mag.* **4**, 451 (1959).
10. Supported by the Petroleum Research Fund of the American Chemical Society and the NSF.

13 April 1964

Strain-Induced Birefringence in Fluoride Films on Uranium Dioxide

Abstract. *Optically birefringent microstructures are formed within fluoride films that are produced on uranium dioxide by hydrofluorination. The positive molar volume change of the reaction produces nonuniform tensile and compressive stresses around sites of surface roughness which result in optical double refraction.*

Moyer and Ochs (*1*) have recently studied the optically birefringent spherulites within polymer films by microscopy and tritium autoradiography. Their photomicrographs taken with polarized light show superficial similarity to features also seen in surface films produced by gas-solid reactions. We have observed analogous doubly refractive microstructures within fluoride films formed on polished surfaces of uranium dioxide by hydrofluorination. These latter growth features appear to be the result of nonuniform lateral stresses originating within the film around sites of nonplanar surface topography (*2*).

Hydrofluorination reactions were performed in a nickel reaction chamber under controlled conditions of pressure, time, and temperature. The materials and apparatus were described earlier (*3*). The product films were examined on a Bausch and Lomb research metallograph and on a Zeiss metallurgical microscope. Figure 1*A* shows a photomicrograph taken with a bright-field illumination and a 5550-Å filter of a film 2 μ thick formed on a flat, polished surface of UO_2 (solid) by reaction with HF (gas) at 60 cm-Hg and 286°C for 90 hours. Nonuniformity of thickness is evident from the interference bands along the scratch and around the hillocks and pits. The smooth area is thicker than the surrounding regions so that the bands indicate a progressive thinning away from the flats. This was demonstrated by a tilt in the interference filter which shifts the transmitted wavelength from 5550 Å to the blue. The bands are thus observed to move away from the flats, and, in the case of the circular nonuniformities, to close in upon themselves. This observation was confirmed by the same tilt-shift in a wedge formed in the film by a scratch mark. Figure 1*B* shows the same area as in Fig. 1*A* but was photographed with crossed polarizers. Three distinct features can be correlated with Fig.

1A. (i) Spherulitic structures correspond to the circular nonuniformities. (ii) Parallel bands are shown along the scratches. (iii) Optical anisotropy is absent from the grain flat. The structures in Fig. *1B* are only very faintly visible when viewed with polarized white light without an analyzer. By using a 50 × apochromatic objective with an open aperture diaphragm, it is possible to distinguish between features within the bulk of the film and on the surface. By this method it can be seen that the optical anisotropy in Fig. *1B* results from an internal layered structure occurring in sheets close to, but not always at, the substrate-film interface.

This structure is further demonstrated by examining thickly coated microcrystals. Figure *1C* shows a photomicrograph taken with bright-field illumination of an annealed fragment of UO_2 (solid) that was reacted with HF (gas) under conditions similar to those of the specimen shown in Fig. 1 *A* and *B*. The reacted fragments were mounted in plastic, lapped with 0.25-μ diamond paste on silk cloth, and inspected metallographically. Layer *1* is viewed in the plane of the film-substrate interface and layer *2* is viewed at an oblique angle. Figure *1D* shows the same specimen photographed with crossed polarizers. Strong optical birefringence is seen in layer *2* but not in layer *1*. Prior to being mounted, these coated crystals were optically anisotropic with a uniform distribution over the entire surface so that anisotropy is present in layer *1* but it is not seen. All of several microcrystals inspected this way exhibited the same appearance. This observation is explained if the double refraction originates in a thin sheet approximately parallel to the film-substrate interface.

The birefringence appears to be a result of the compressive and tensile forces that develop during the formation of the product around nonplanar configurations in the surface of the substrate. Figure 2 shows an idealized product layer as formed around a positive (that is, raised) feature in the substrate. The molar volume ratio of UF_4 (solid) to UO_2 (solid) is 1.90 and the deposition of product apparently takes place at the product-substrate interface through inward migration of the reactant gas (*3*). Thus tension would occur at apex *2* with compression along lines *1*. The forces would be reversed for a negative surface feature, for example, an etch pit.

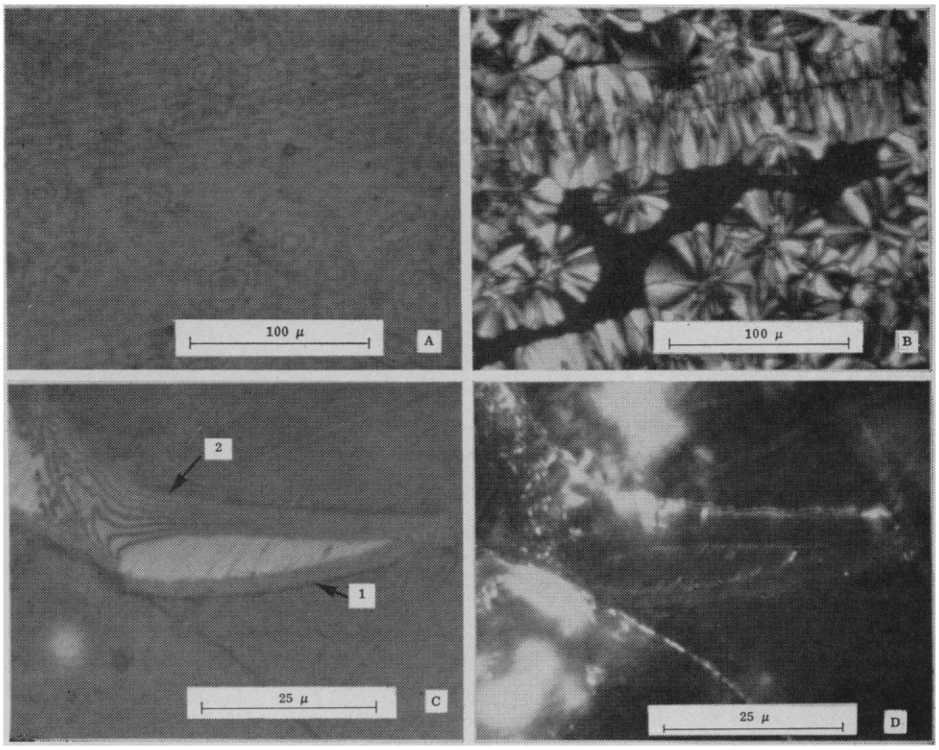

Fig. 1. Photomicrographs of fluoride films produced on uranium dioxide by hydrofluorination; (left) bright-field illumination and (right) crossed polarizers. *A* and *B* show a flat, polished specimen and *C* and *D* show a microcrystalline fragment. Layer *1* in *C* is viewed in the plane of the film-substrate interface and layer *2* is viewed at an oblique angle.

As a test of this proposal, the directions of vibration of the fast and slow components were determined with a first-order red plate. The gradations in intensity in Fig. *1B* suggest that the vibration directions change smoothly within the substructures that radiate outwardly from a common source. The slow direction, γ, is approximately parallel to the radius vector in the round structures and is perpendicular to grain boundaries. There are variations, of course, within these contiguous, granular structures. A birefringence of 0.03 ± .01 was measured with a Berek compensator. This value is within the limits of 0.044 reported by Staritzky (*4*) and of 0.096 reported by Shankar *et al.* (*5*) for monoclinic UF_4 (solid) at λ_D. Thus these features may represent either strain birefringence or perhaps a strain-induced recrystallization of the product layer.

As a parallel observation, a sheet of silver chloride 10 mil in thickness was

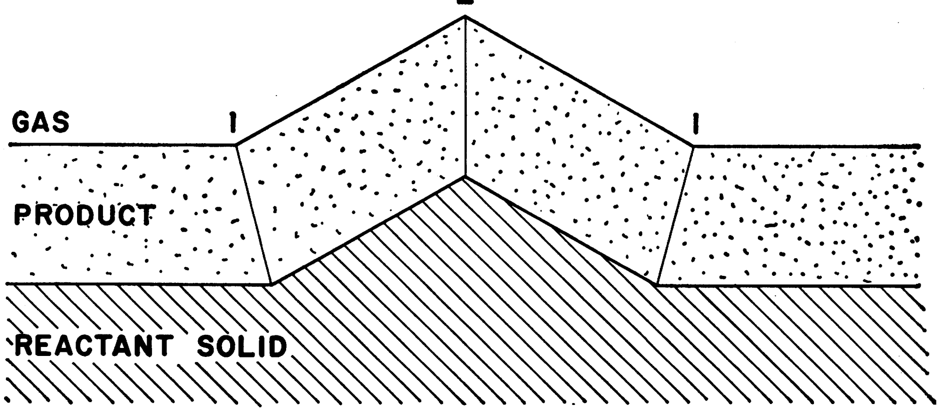

Fig. 2. Formation of product around a raised feature in the substrate.

stretched beyond its elastic limit. Within a freshly stretched sheet remain discrete birefringent substructures in which the slow direction is parallel to the direction of the tensile stress. Stretched sheets of polyethylene or rubber also exhibit birefringence in which the slow direction is parallel to the applied force. Thus the birefringence of Fig. 1*B* is consistent with a film which has been thinned by tensile stresses.

W. P. ELLIS

Los Alamos Scientific Laboratory,
Los Alamos, New Mexico

References and Notes

1. J. D. Moyer and R. J. Ochs, *Science* **142**, 1316 (1963).
2. For a discussion of strain birefringence, see E. M. Chamot and C. W. Mason, *Chemical Microscopy* (Wiley, New York, ed. 3, 1958), vol. 1, pp. 195, 289, 335; and G. K. T. Conn and F. J. Bradshaw, *Polarized Light in Metallography* (Academic Press, New York, 1952), p. 78.
3. W. P. Ellis and B. W. Roberts, *J. Chem. Phys.* **39**, 1176 (1963).
4. E. Staritzky and A. L. Truitt, in *The Actinide Elements*, G. Seaborg and J. Katz, Eds. (McGraw-Hill, New York, 1954), p. 813.
5. J. Shankar, P. G. Khubchandani, V. M. Padmanabhan, *Anal. Chem.* **29**, 1374 (1957).
6. Based on work performed under the auspices of the U.S. Atomic Energy Commission. I thank R. M. Douglass for assistance with the compensators.

30 March 1964

Alloocimene: Absence in Cigarette Smoke

Abstract. *Alloocimene was not found to be a constituent of cigarette smoke under test conditions that allowed 86 percent recovery when authentic alloocimene was added to the smoke. In the same experiments dipentene was found to the extent of 0.2 percent of the smoke condensate.*

Wynder and Hoffmann recently reported (*1*) the presence of "up to 0.5 percent alloocimene" in cigarette smoke. These authors also found that alloocimene (2,6-dimethylocta-2,4,6-triene) was an effective promoter of mouse skin carcinogenesis when applied in a concentration of 1 to 5 percent after an initiating dose of 300 μg of dimethylbenzanthracene.

Studies in our laboratory have failed to show the presence of alloocimene in smoke from cigarettes made with a blend of Bright (flue-cured) tobaccos or with a typical commercial blend of Bright, Burley, Turkish, and Maryland tobaccos. Our measurements indicate that not more than 2.4 μg of alloocimene could be present in the smoke from one 85-mm cigarette. This is equivalent to less than 0.006 percent of the smoke condensate.

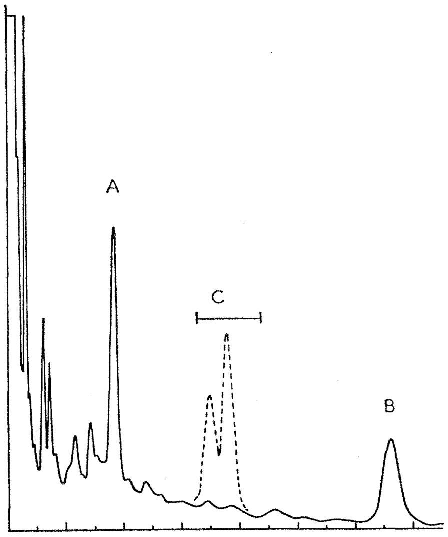

Fig. 1. Gas chromatogram of a volatile extract of cigarette smoke. *A*, Dipentene. *B*, Octyl iodide (190 μg per cigarette, added). *C*, Effluent range collected for ultraviolet examination. The dashed curve under *C* shows the response obtained when 186 μg of alloocimene per cigarette was added to the smoke traps.

Although we were unable to find any evidence for alloocimene in cigarette smoke, we did confirm the presence of dipentene to the extent of 76 to 108 μg in smoke from 85-mm cigarettes made with the commercial blend of tobaccos and 164 to 180 μg in smoke from 85-mm cigarettes made with a blend of Bright tobaccos. This is equivalent to average values of 0.2 and 0.3 percent of the respective smoke condensates. Dipentene was previously reported as a constituent of cigarette smoke by Johnstone *et al.* (*2*).

The cigarettes were smoked to a constant butt length of 30 mm in the Liggett and Myers' Model 4 smoking machine (*3*) that took ten puffs of 2 seconds each at 60-second intervals. The smoke was condensed in glass traps cooled with liquid air. Smoke condensate from 105 cigarettes (85-mm) was rinsed from the traps with three 25-ml portions of distilled water and four 25-ml portions of cyclopentane. Each of the cyclopentane rinses was used in turn to extract the combined water fraction. The cyclopentane extracts were then combined and concentrated at 25°C with a stream of nitrogen to a volume of 10 ml. This solution was distilled at 95°C at a pressure of 1.0 mm-Hg and the distillate was collected in an efficient glass-coil trap cooled in liquid air. The distillate was diluted to 10 ml with cyclopentane and a 5-μl portion was analyzed by gas-liquid chromatography at 80°C on a 0.5 cm (ID) by 1.8 m stainless-steel column containing 80 to 100 mesh Gas-Chrom P (*4*) coated with 6 percent silicone rubber, SE-30 (*4*). Helium carrier gas at 2.6 atm inlet pressure was used to provide an exit flow rate of 90 cm^3/min. The instrument used for the gas-liquid chromatography was equipped with dual columns and flame ionization detectors (*5*).

Octyl iodide was added to the smoke traps before collection of the sample, to provide an internal standard from which completeness of recovery could be estimated. For several determinations the recovery of octyl iodide ranged from 84 to 88 percent. No definite indication of alloocimene was obtained in the gas chromatogram at a retention time typical of authentic alloocimene (Fig. 1). Since there was some nonspecific background material eluted from the gas-liquid chromatographic column at the retention time (R_t) for alloocimene, this material was collected (R_t, 6.6 to 8.8 minutes) and examined for intensity of ultraviolet absorption at 220 to 370 mμ. The spectrum for the collected sample was not indicative of alloocimene (*6*). A calculation of amount was made based on the absorbance at 273 mμ. With a value for an intensity of E_{mol} equal to 41,500 at 273 mμ for authentic alloocimene [30 percent *trans*-(C_4)-*trans*-(C_6), 70 percent *trans*-(C_4)-*cis*-(C_6)] and correcting for losses sustained in the collection, we determined that no more than 2.4 μg of alloocimene per 85-mm cigarette could be present in the smoke sample.

In several experiments we added a measured amount of authentic alloocimene (186 μg per cigarette) to the smoke traps before collecting the smoke, to establish the efficiency of our analytical procedure and to determine whether alloocimene was sufficiently stable in the presence of other smoke components. The added alloocimene was recovered from the gas-liquid chromatography to the extent of 86 to 89 percent based on peak area measurement. The *trans-trans* and *trans-cis* isomers emerged after 7.0 and 7.6 minutes, respectively, under the chromatographic conditions used.

The authentic sample of alloocimene